JOURNAL OF MATERIALS SCIENCE **34** (1999) 637–644

Cell nucleation in solid-state polymeric foams: evidence of a triaxial tensile failure mechanism

M. R. HOLL, V. KUMAR‡, J. L. GARBINI‡, W. R. MURRAY‡
Departments of Bioengineering and ‡Mechanical Engineering, University of Washington
Seattle, Washington 98195
E-mail: holl@u.washington.edu

The mechanism for nucleation phenomenon in solid-state microcellular foams is identified as a solid-state failure process. This process originates at internal flaws within the gas-polymer matrix, where it is induced by the presence of a state of hydrostatic tensile stress within the polymer matrix. The hydrostatic tensile stress is caused by the presence of the saturating gas within the polymer. The nucleation phenomenon is thermally activated at the effective glass transition temperature of the gas-polymer mixture. At this critical temperature, the hydrostatic tensile stress within the gas-polymer mixture is sufficient to cause the polymer matrix to fail, thereby creating a foam cell nucleus. In general, the nucleation sites are observed to be flat, approximately circular, fracture sites. After the appearance of the initial fracture, gas diffuses from the gas-polymer matrix into the fracture. The fracture seam inflates during the growth process, in which growth begins with the appearance of a disk shaped fracture and concludes with an approximately spherical cell. The results and conclusions presented herein suggest a new avenue to explain the cell nucleation phenomena observed in this process.

Nomenclature

T	temperature of the specimen (°C)
$T_{g,eff}$	effective glass transition temperature (°C)
T_n	nucleation threshold temperature (°C)
C	gas concentration within the polymer specimen (mg/mg)
C_{ini}	initial gas concentration level of the gas-polymer mixture (mg (gas)/mg (polymer))
ΔV	change in polymer volume due to the presence of the saturating gas (m^3)
V_0	initial volume of the polymer volume prior to gas saturation (m^3)

Subscripts:

net	the net dilation strain due to internal and external hydrostatic stresses
HT	hydrostatic tension
HC	hydrostatic compression
H	hydrostatic stress

1. Introduction

Microcellular foams produced using the solid-state process have extremely small individual cells, in the range of 2–25 μm in diameter. By contrast, other foam production processes produce individual foam cells that are on average greater than 100 μm in diameter and in many cases will exceed 1000 μm (1 mm). The small cells produced by the solid-state microcellular process qualify microcellular foams for a number of unique application areas. Some examples are the production of parts with very thin walls, machinable bulk foam stock, and engineered integral plastic composites.

In the solid-state microcellular process, a solid thermoplastic polymer is placed in a pressure vessel and exposed to an inert gas under high pressure. The concentration of the gas within the polymer is determined by the diffusion dynamics of gas into the polymer. After a sufficiently long time, the polymer acquires a uniform gas concentration level throughout its cross-section. In this fully saturated condition, the polymer exhibits a volumetric expansion due to the presence of the gas. This expansion is referred to as a gas-induced polymer dilation. Upon removal of specimens from the high pressure saturation environment, a net state of hydrostatic tensile stress in the polymer is known to result from this dilation strain. The gas-saturated specimen, once removed from the pressure vessel, is heated. The increase in temperature causes a drop in mixture strength. At a critical mixture temperature, the state of tensile stress within the polymer matrix causes rupture of the polymer matrix at numerous locations. Gas diffusion from the mixture surrounding the nucleation sites provides the driving force for cell growth.

Microcellular plastics have been produced using the solid-state method in several gas-polymer systems. The inert gases used are predominately nitrogen (N_2) and carbon dioxide (CO_2). The polymers to which the solid-state process have been applied are polystyrene (PS), high impact polystyrene (HIPS), polyethylene terephthalate (PET), polycarbonate (PC), polyvinylchloride

(PVC), polymethylmethacrylate (PMMA), and acrylonitrile-butadiene-styrene (ABS).

1.1. Previous work on nucleation phenomenon in solid-state microcellular plastics

The microcellular process was developed at MIT in the early 1980s redefining a similar process described by IBM researchers in the 60s [1]. Martini used this process produce foam in high impact polystyrene sheets using nitrogen and carbon dioxide as the inert saturating gas [2–4]. Martini performed experimental work to assess the relative mechanical strength of the foams produced and derived models for cell nucleation and growth. Martini concluded that classical nucleation theory is not directly applicable to the solid-state process [2].

Following Martini's lead, a number of researchers have focused their attention on the nucleation phenomenon in microcellular systems. Colton [5–8] studied bubble nucleation in the nitrogen-polystyrene system, with and without various nucleating agents. He proposed nucleation models built around classical nucleation theory that dates back to J.W. Gibbs. Colton suggests that additives do not exist as second-phase particles at very low additive concentrations and therefore do not provide sites for heterogeneous nucleation. In this case, homogeneous nucleation occurs within the free volume of the polymer. Conversely, at additive concentrations above the solubility limit of the polymer Colton concludes that additives do exist as distinct second-phase particles and are advantageous nucleation sites for heterogeneous nucleation to occur. This correlates qualitatively with a critical second-phase size argument presented by Ramesh *et al*. [9].

Kweeder *et al.* [10] of Clarkson University suggested that nucleation occurs at pre-existing microvoids resulting from previous processing history of the polymer. This hypothesis followed from the work of Adams [11], who concluded that prior processing history can cause significant addition of very small cracks or microvoids in the polymer matrix.

Ramesh further investigated nucleation in the polystyrene (PS) and high impact polystyrene (HIPS) system using nitrogen and carbon dioxide as the physical blowing agents [9]. The focus of this research was to experimentally investigate the hypothesis that the elastomeric inclusions in the HIPS acted as nucleation sites. Ramesh concluded that 2 μm inclusions provided excellent nucleation sites. However, below a critical radius, Ramesh observed that the elastomeric inclusions were not effective as nucleation sites. In further work on this topic, Ramesh combined the earlier work of Kweeder with the concept that the elastic forces in the polymer matrix are significant in the transition from a microvoid to a viable bubble [12–14]. In this work, Ramesh concluded that including elastic forces, surface forces and widely differing glass transition temperatures between the polymer matrix and the included particulate was responsible for the observed nucleation phenomenon. The Ramesh nucleation model does not address the plasticizing effect of the gas present in the polymer matrix upon the elastic modulus of the gas-polymer mixture.

In this paper, we first discuss the effects of plasticizing gases on polymers and then propose a new mode of cell nucleation specific to the solid-state process, where the creation of cell sites occurs while the polymer is in a solid-state and the cell sites originate as internal fractures. Second, we review a closely related body of research associated with failure of elastomeric composites. Finally, we present experimental evidence of the failure process responsible for cell nucleation in microcellular polycarbonate.

1.2. Polymer plasticization and gas-polymer interactions

Plasticization of polymers by the addition of a low-glass-transition second-phase polymer or a plasticizing solvent is a well documented phenomenon [16, 17] that causes the following effects: (1) small depression in the apparent polymer melting point; (2) significant depression in the effective glass transition temperature; (3) significant depression in the effective yield stress of the mixture; (4) increase in both the effective yield strain and the percent elongation at break; and (5) significant decrease in the effective viscosity of the melt. The glass transition temperature is representative of the temperature at which the polymer shows the first significant sign of polymer mobility [18]. The behavior of gas-saturated plastics have been shown to exhibit excellent correlation with the published behavior of plasticizer systems. This is best documented for effective glass transition temperature [19–27]. Fig. 1 illustrates the general strength versus temperature behavior of gas plasticized amorphous thermoplastics.

In Fig. 1, three strength curves are shown for three different gas concentration levels ($C_{\text{ini},4} > C_{\text{ini},3} > C_{\text{ini},2}$). The higher the gas concentration level, the larger the shift of the strength curve to the left. The precipitous drop in mixture strength occurs near the effective glass transition temperature of the mixture. In addition to any external stresses placed upon the specimen, a state of triaxial tensile stress exits due to the presence of the saturating gas. Evidence of this state of stress and strain is observed by measurement of volume dilation. The dilation phenomenon (polymer swelling) exhibited by specimens raised to high equilibrium gas concentration levels (via high exposure pressures) has been reported by several investigators in polycarbonate and polycarbonate blend systems [28–32].

The correspondence of the phenomenon of cell nucleation in solid-state microcellular systems to the presence of gas is related to a similar phenomenon known as *explosive decompression failure*, which is observed in elastomers and plastics used in high pressure environments [33]. In this phenomenon the elastomers exhibit internal failure and rapid fracture expansion when rapidly depressurized.

Gent and Lindley [34] examined the internal rupture of bonded rubber cylinders in tension using the *poker chip* test. In the poker chip test, a nearly uniform

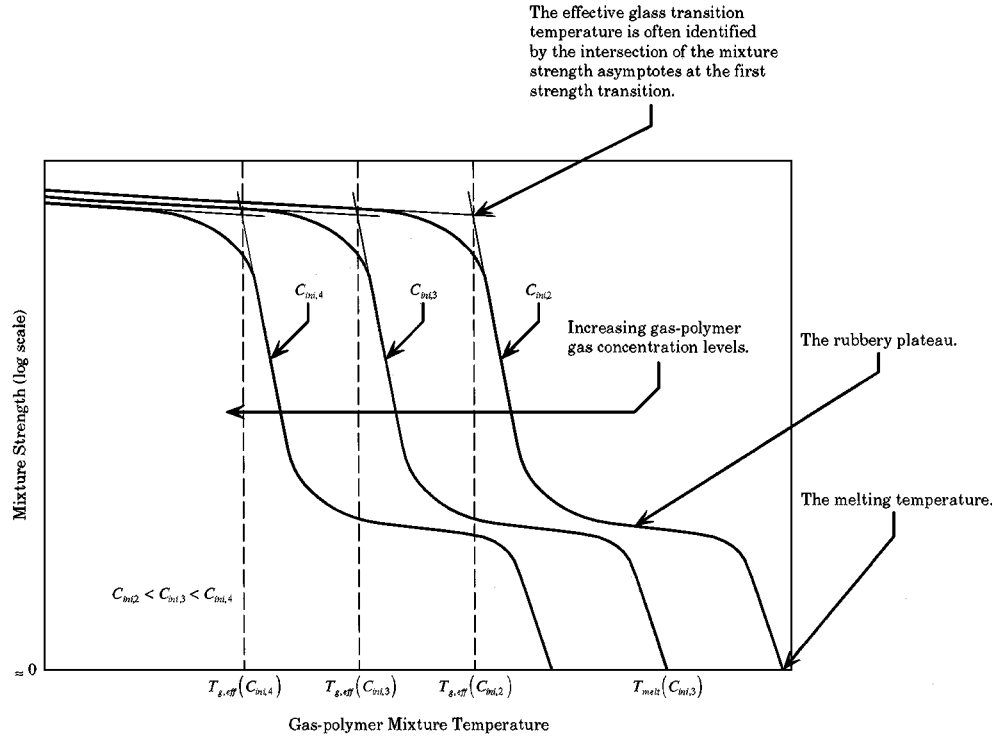

Figure 1 Illustration of the strength of gas-polymer mixtures as a function of temperature and gas concentration level.

state of triaxial tension is produced at the center of the test specimen. Their experimental parametric study provided a characterization of the failure modes exhibited as a function of the hydrostatic tensile (HT) stress field intensity. The failure phenomenon produced by the HT field was observed to be a dense set of randomly oriented circular cracks.

Williams and Schapery in 1965 [35] examined the stability of spherical inclusions in an elastic body subjected to a HT stress field. Their theoretical work examined the limiting behavior for very small and very large cavities and correlated the results to existing critical stress values for material fracture.

In 1967 Lindsey [36] published a study containing both theoretical and experimental components examining the triaxial tensile failure characteristics of a polyurethane using the poker chip test. The nucleation sites observed were circular, planar cracks that were theorized to initiate at small entrained air pocket within the cast urethane specimens.

The correlation between internal flaw size and the hydrostatic tensile stress required for matrix failure was examined analytically by Gent and Tomkins in 1969 [37]. Their analysis lead them to the conclude that small holes with radii of 10 Å or so require very high stress levels in order to overcome both the elastic and surface energy restraining fracture growth as expected for such small defects, where surface energy forces dominate.

Later in 1969 Gent and Tomkins presented an experimental work [38] expanding on their earlier analytic work [37]. In this experimental work, a butadiene-styrene copolymer was saturated with carbon dioxide maintained at two different fixed high pressures on opposite sides of each test specimen. The specimens attain a gas concentration that varies linearly across the specimen in the steady-state. They assumed that upon release of the external gas pressure, triaxial tensile stress varies linearly across the specimen. Flaws with the copolymer of sufficient size acted as initiation sites for rapid cell expansion. Tearing of the elastomer matrix was also observed. In this study, Gent and Tomkins also observed the expansion of small satellite bubbles formed around a single large expanding central bubble. Gent and Tomkins concluded that good agreement between the analysis predictions and experiment was observed.

Briscoe and Zakaria examined the phenomenon of damage produced in elastomers exposed to high gas pressures and then exposed to rapid decompression [33, 39, 40]. Their experiments were performed using DOW Sylgard S-184 silicone polymer. Various fillers were used in their experiments with both treated and untreated surfaces to alter the bonding efficiency of the Sylgard to the filler material. A significant conclusion of the research of Briscoe and Zakaria was that if failure can be induced to occur at many sites the resulting failure fractions will be smaller and evenly distributed throughout the matrix.

This body of experimental and theoretical work provides the foundation supporting our association of a new mechanism of cell nucleation with solid-state microcellular systems.

2. Proposed mechanism for solid-state cell nucleation

2.1. Hydrostatic tension in gas-polymer solutions

We propose a mechanism for cell nucleation in the solid-state microcellular process that is the result of

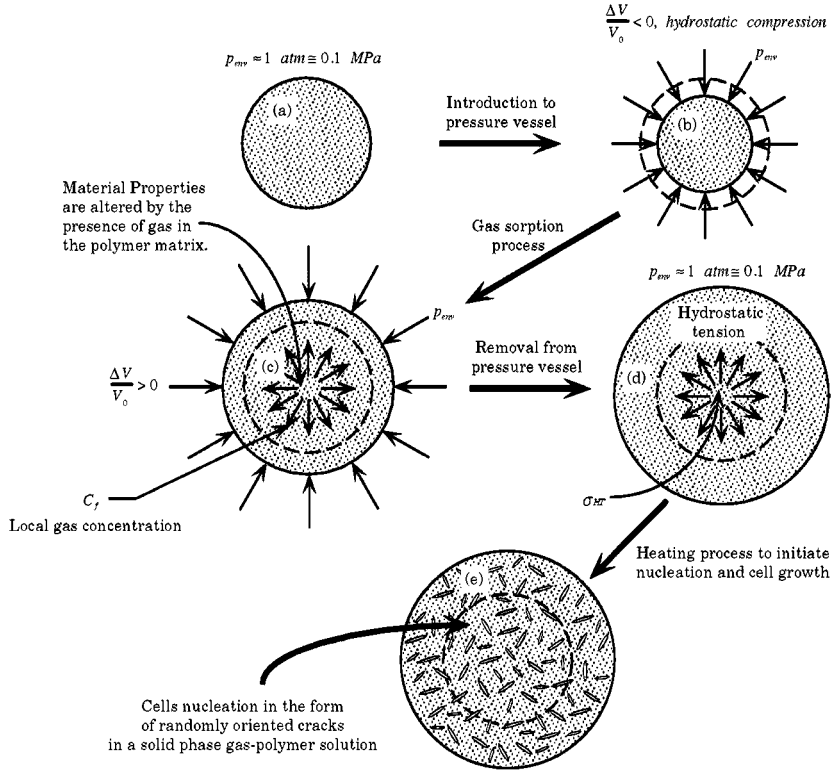

Figure 2 Equilibrated states in a gas-polymer system up to the nucleation of void in the mixture.

a hydrostatic tensile stress in the polymer matrix in excess of the material strength. This proposed mechanism is similar to mechanisms presented in a body of work performed by researchers in the field of elastomer failure in high gas pressure environments upon rapid decompression. As suggested by Briscoe and Zakaria [33], gas-polymer solutions below their effective glass transition temperature do not possess the required chain mobility to expand in the presence of the stresses in the polymer that cause swelling. Therefore, these gas-polymer solutions exist in a state of triaxial tension. Fig. 2 illustrates the processing steps with the polymer matrix during solid-state processing up to the void (cell) nucleation event.

The process begins with a gas-free polymer, Fig. 2a. The polymer is placed in a pressurized environment and initially experiences a hydrostatic compression, Fig. 2b. As gas diffuses into the specimen, the gas-polymer mixture expands and a net positive volume expansion is observed, Fig. 2c. The gas-saturated specimen is removed from the high pressure environment and returned to atmospheric pressure resulting in further volume expansion, Fig. 2d. When heated the mixture strength decreases while still remaining solid and a dense population of internal fractures appear in the solid, Fig. 2e.

Once cell nucleation is activated, gas will leave the gas-polymer mixture to fill growing cells. This gas depletion will reduce the local state of polymer swelling and, therefore, the state of local hydrostatic tension. Because the local state of hydrostatic tension is decreased, the driving force for cell nucleation is diminished. The loss of gas from activated cells with time suggests a critical dependence of cell nucleation density upon the rate of gas-polymer mixture temperature increase.

3. Experiment

3.1. Foam specimen preparation

GE LEXAN®9030 polycarbonate specimens, 1.5 mm thick and machined to 31 mm in diameter from extruded sheet stock, were exposed to 4.83 MPa carbon dioxide gas at 25 °C. The specimens were maintained in the pressurized carbon dioxide environment until an equilibrium, uniform, gas concentration profile was achieved (approximately 72 h). The gas saturation level at equilibrium was determined to be 0.0874 mg (CO_2)/mg (PC), nominal. Small fluctuations in gas saturation level occurred due to variations in ambient temperature (±6.0 °C) and environmental gas pressure (±0.21 MPa).

Each saturated specimen was immersed in the heated glycerin bath at the desired temperature for the predetermined length of time, and then quenched in ice water to arrest cell growth. Five different glycerin bath temperatures were examined for the foam growth experiments: 60 °C, 80 °C, 100 °C, 120 °C, and 140 °C (±0.1 °C). A set of desired foaming times (±0.5 s) was tabulated prior to foaming the saturated specimens. Foaming times were more tightly clustered at short foaming times when the nucleation process was expected to occur. For each of the five glycerin bath temperatures examined, the process was repeated for incrementally longer foaming times on specimens with the same initial geometry and gas saturation level.

3.2. Preparation of foam specimens for SEM micrographs

Traditional characterization of foam structure examines the fracture surface produced by snapping specimens quenched in liquid nitrogen. The fracture surface

propagates through the specimen following a random path determined by internal flaws and weak zones in the foam structure [43].

The random surface, though useful for rapid examination of general foam characteristics, does not define a true planer test probe, which is desirable for quantitative assessment of foam structure from SEM micrographs (e.g., estimation of local foam void fraction) [43, 44].

We fabricated a device that allowed planer surfaces to be produced in the polycarbonate foams. The basic principle of operation for the apparatus requires that a cleaving blade be passed through a foam specimen to produce the desired test surface. The blade is held stationary and the specimen is moved relative to the blade with a relative motion having a component directly into and tangent to the blade edge. During normal use the specimen is moved relative to the razor blade in the specimen feed direction at a rate of approximately 130 μm/s until the razor edge has passed through the specimen completely. The specimen is then dropped away from the blade and removed from the specimen holder. All specimens were severed using a new razor blade edge. The severed surface is sputter coated with Au-Pd and examined using a scanning electron microscope (SEM). Fig. 3 shows a comparison of the surfaces produced by the liquid nitrogen quench/snap and razor blade preparation procedures.

Images shown in the left column of Fig. 3 demonstrate the random fracture surfaces produced by the liquid nitrogen quench/snap procedure. The planer surfaces produced using the razor blade severing method are shown in the right column of Fig. 3. Each of the three micrographs in the right column show planar surfaces with clearly defined cell edges. No cell distortion is observed in the micrographs prepared from severed specimens. The images in each row of Fig. 3 were taken from the center of a single foam specimen. However, the images in the left column appear to have more void space than their severed counterparts in the right column. Two factors contribute to this effect. First, a random fracture

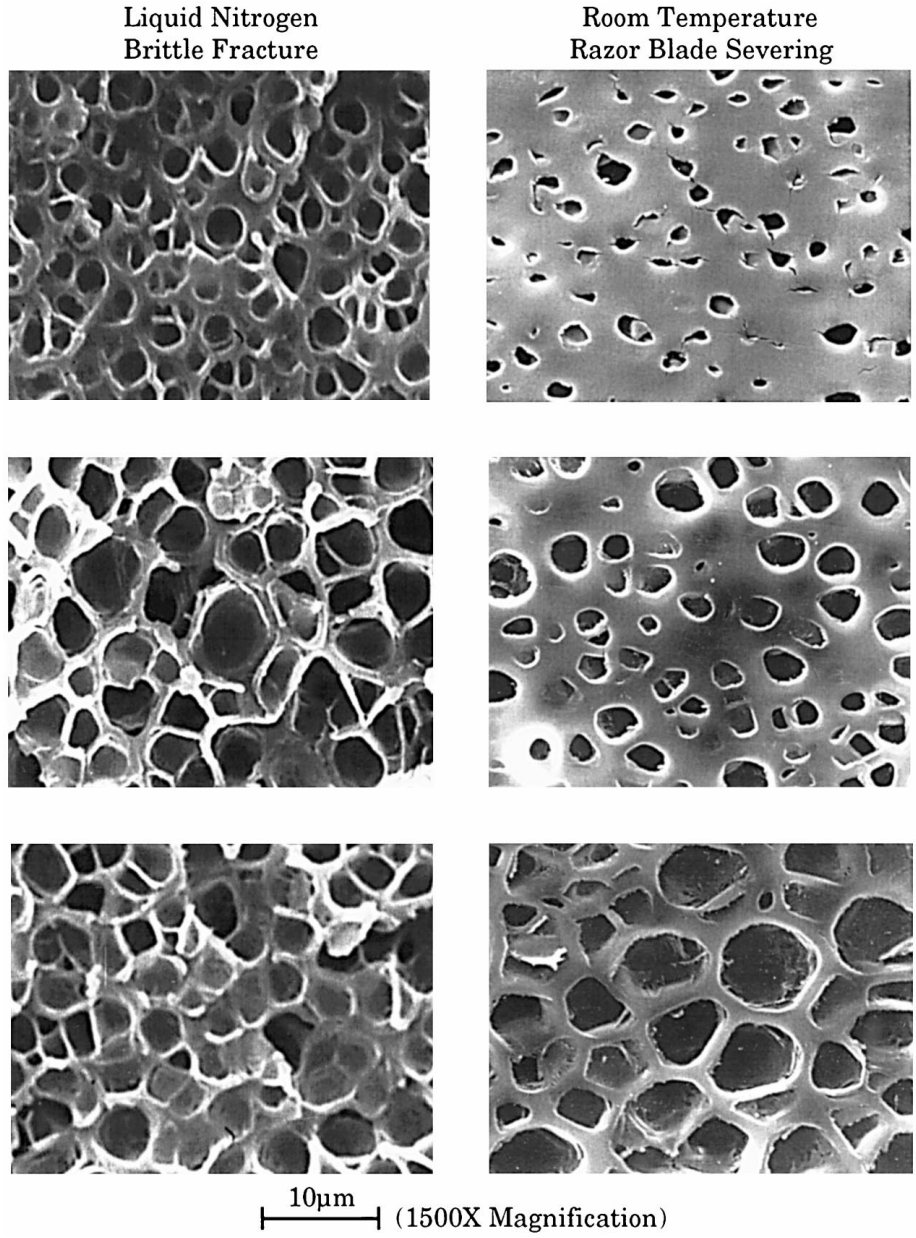

Figure 3 Comparison of planer intersection surfaces produced in various foam microstructures using the traditional liquid nitrogen quench/snap procedure and the razor blade severing procedure.

surface will propagate through the foam following a path defined by minimum strength and will therefore selectively propagate through a path within the foam with the minimum solid material. Whereas, a planer section is constrained to pass through solid material as well as the void space of the foam cells. Second, small location-to-location variations in foam structure are observed in polycarbonate solid-state foams. Methods of quantitative stereology, used for the assay of three dimensional structure from two dimensional images, require images of planer specimen sections [44]. During specimen preparation, 20% of the specimens prepared exhibited cell distortion and were not used. The cell distortion in polycarbonate foams was traced to inconsistent quality of the razor blade edge.

4. Results and discussion

Fig. 4 shows the SEM images of foam structure at exposure times during the foaming process very near the time nucleation occurs for foaming temperatures of 60, 80, 100, 120, and 140 °C. Data correlating changes in foam density to foaming temperature demonstrate that nucleation occurs when the temperature of the mixture is nearly equal to the effective glass transition temperature (see Fig. 1).

Two process characteristics of Fig. 4 are important to note. First, nucleation is observed at longer exposure times for lower exposure temperatures. Second, fewer void nucleation sites are observed at lower exposure temperatures and these sites are significantly larger than those produced at higher temperatures. Examination of Fig. 4a reveals that void fraction appears in the polymer in the form of *cracks*. The cracks, shown at all foaming temperatures, provide evidence of a fracture process associated with the nucleation. If the mixture is maintained very close to the effective glass transition temperature, Fig. 4a, it appears that relatively few regions in the gas-polymer mixture are sufficiently weak for the state of tensile stress to initiate internal matrix rupture. However, once a failure zone is initiated at a preferential site, then the fracture surface is observed to propagate through the foam along the polymer sheet orientation plane. Because few sites activate, the gas available goes to the limited number of fracture sites and these cracks become quite large. Examination of Fig. 4b shows cracks that develop in foams produced at 80 °C where the largest cracks are shorter than those produced at 60 °C, and many very small fracture cracks are observed as well. We believe that a larger number of triaxial tensile fracture sites are activated if the mixture is heated fast enough and to sufficient extent beyond the effective glass transition temperature. The net effect of this internal failure throughout the mixture is to diminish the state of triaxial tensile stress in the matrix rapidly and uniformly. This rapid and uniform reduction of the triaxial tensile stress field is hypothesized to impede the propagation of large cracks in favor of many smaller cracks.

The fracture cracks exhibited at 100 °C, Fig. 4c, shows a transitional departure from the behavior observed in the 60 °C and 80 °C. At 100 °C the failure cracks are between 0.25 and 3 μm in length and are distributed with greater uniformity throughout the polymer matrix than the one or two order of magnitude larger cracks observed for 60 °C and 80 °C. In the 100 °C

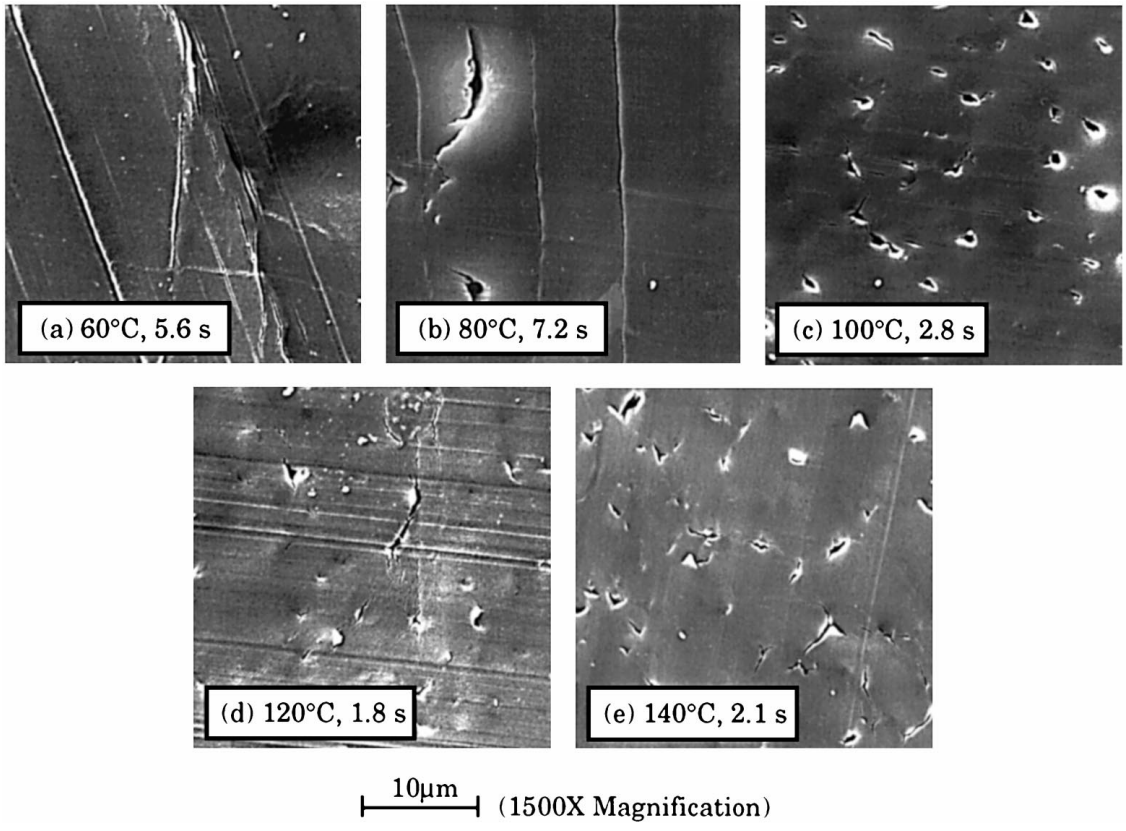

Figure 4 Nucleation phenomenon in the PC-CO2 solid-state foam process. All micrographs were taken at the specimen centerline.

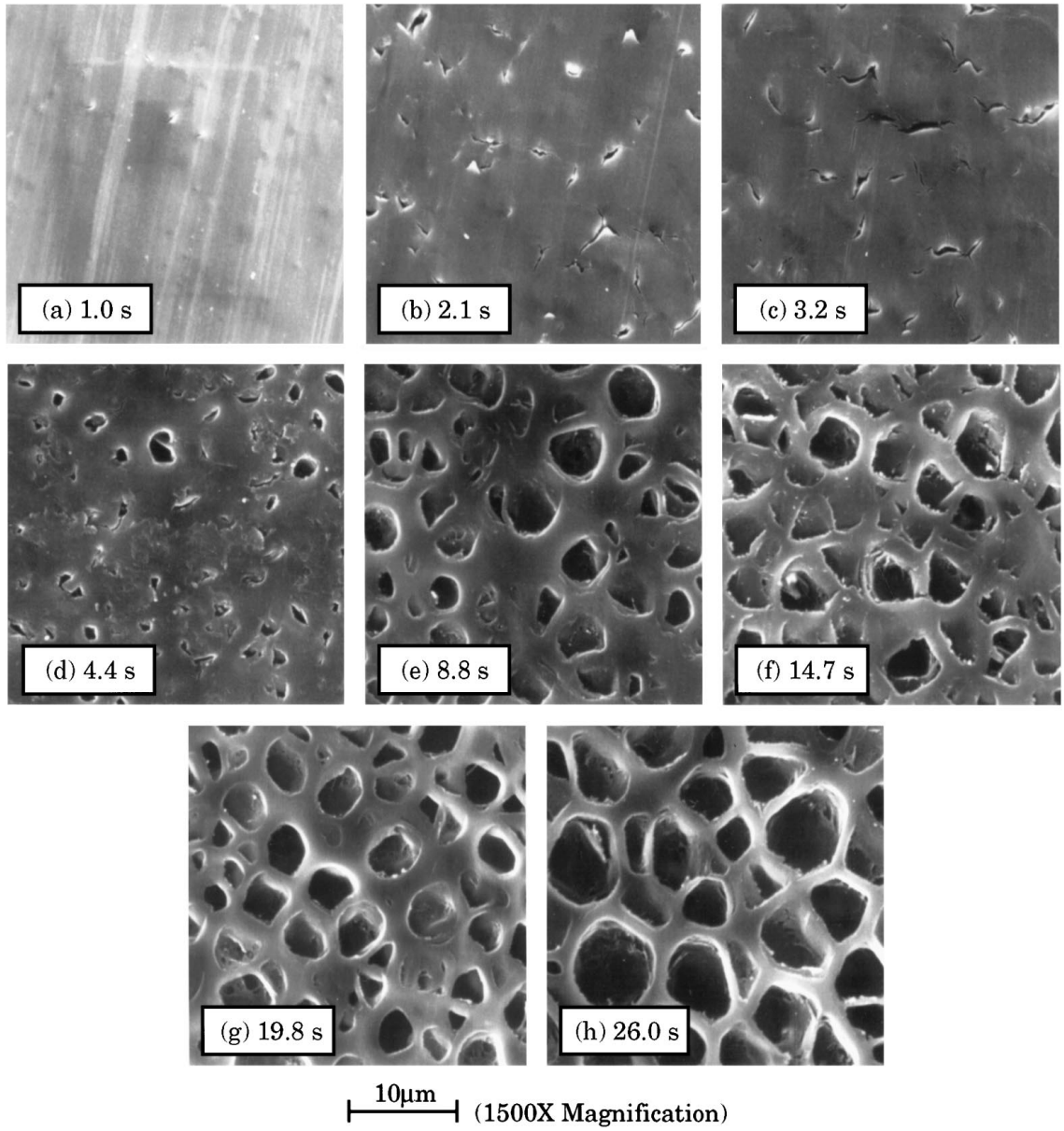

Figure 5 Dynamic cell growth response at the specimen centerline in a 140 °C heated glycerin bath.

specimen, significant regions exist in the mixture where no localized fractures in the form of cells, cracks, or seams are observed.

At 120 °C and 140 °C, Fig. 4d and e, small fractures less than 3 μm in length are densely packed within the volume. We believe this is due to the rapid heating of the specimens and the dramatic decrease in strength over short time period.

Fig. 5 presents the dynamic growth sequence at the centerline of the 1.5 mm thick specimens prepared at 140 °C. Observation of the change in cell geometry with time shows that cells with a high degree of spherical symmetry begin as individual cracks produced in a solid polymer matrix.

5. Conclusions

Prior work dealing with nucleation phenomenon in microcellular plastics has assumed that cells begin as spherical microvoids present in the native polymer or caused by the addition of approximately spherical second-phase additives [3, 8, 13, 14], and that this spherical shape is maintained throughout the cell growth process. Our research indicates that in the solid-state process cells originate from cracks that appear to be the result of a fracture process [43]. A body of literature in the related field of failure of elastomers provides supporting theory and phenomenological evidence. The internal fracture process we observe in solid-state microcellular materials, in general, generates randomly oriented cracks in the mixture with length less than 3 μm. In all cases, cell nucleation occurs when a solid gas-polymer mixture is heated to within a few degrees Celsius of the effective glass transition temperature. Where, at this temperature, a precipitous drop in mixture strength occurs for amorphous thermoplastics. Thus, the cell nucleation phenomenon in the solid-state microcellular process is essentially a triaxial tensile failure process.

Acknowledgements

This research was supported in part by grants from the National Science Foundation, the Washington Technology Center, the University of Washington Royalty Research Fund, and the UW-Industry Cellular Composites Consortium.

References

1. E. J. BARLOW and W. E. LANGLOIS, *IBM J. Res. and Dev.* **6** (3) (1962) p. 329–337.
2. J. E. MARTINI, The production and analysis of microcellular foam, Department of Mechanical Engineering, MIT, 1981.
3. J. MARTINI, F. A. WALDMAN and N. P. SUH, The production and analysis of microcellular thermoplastic foams, SPE ANTEC Technical Papers, 1982. Vol. XXVIII: pp. 674–676.
4. J. E. MARTINI-VVEDENSKY, N. P. SUH and F. A. WALDMAN, Microcellular closed cell foams and their method of manufacture, United States, 1984.
5. J. S. COLTON, The nucleation of microcellular thermoplastic foam, Massachusetts Institute of Technology, Cambridge, 1985.
6. J. COLTON and N. P. SUH, *Polym. Eng. Sci.* **27** (7) (1987) 500–503.
7. *Idbm, ibid.* pp. 493–499.
8. *Idbm, ibid.* pp. 485–492.
9. N. S. RAMESH, *et al*. An experimental study on the nucleation of microcellular foams in high impact polystyrene, in SPE ANTEC 92 (Detroit MI, 1992).
10. J. A. KWEEDER, *et al*., The nucleation of microcellular polystyrene foam, SPE Technical Papers (1991) Vol. 37, p. 1398.
11. M. E. ADAMS and G. A. CAMPBELL, *Polym. Eng. Sci.* **31** (18) (1991) 1337–1343.
12. N. S. RAMESH, D. H. RASMUSSEN and G. A. CAMPBELL. The nucleation of microcellular foams in polystyrene containing low glass transition particles, in SPE ANTEC 93 (New Orleans, 1993).
13. *Idem, Polym. Eng. Sci.* **34** (22) (1994) 1685–1697.
14. *Idem, ibid.* pp. 1685–1697.
15. V. KUMAR, Process synthesis for manufacturing microcellular thermoplastic parts: A case study in axiomatic design, Massachusetts Institute of Technology, Cambridge, 1988.
16. A. K. DOOLITTLE, *J. Polym. Sci.* **2** (2) (1947) 121–141.
17. J. K. SEARS and J. R. DARBY, "The technology of plasticizers" (John Wiley & Sons, New York, 1982).
18. V. L. SIMRIL, *J. Polym. Sci.* **2** (2) (1947) 142–156.
19. R. F. BOYER and R. S. SPENCER, *ibid.* pp. 157–177.
20. T. S. CHOW, *Macromolecules* **13** (1980) 362–364.
21. K. J. BEIRNES and C. M. BURNS, *J. Appl. Polym. Sci.* **31** (1986) 2561–2567.
22. S. KALACHANDRA and D. T. TURNER, *J. Polym. Sci.: Part B, Polym. Phys.* **25** (1987) 1971–1979.
23. W. J. KOROS and D. R. PAUL, *J. Polym. Sci., Polym. Phys. Ed.* **16** (1978) 1947–1963.
24. M. D. SEFCIK, *J. Polym. Sci.: Part B, Polym. Phys.* **24** (1986) 957–971.
25. Y. KAMIYA, *et al., J. Polym. Sci.: Part B, Polym. Phys.* **24** (1986) 535–547.
26. *Idem, ibid.* pp. 1525–1539.
27. *Idem, ibid.* pp. 159–177.
28. G. K. FLEMING and W. J. KOROS, *Macromolecules* **19** (1986) 2285–2291.
29. M. D. SEFCIK, *J. Polym. Sci.: Part B, Polym. Phys.* **24** (1986) 935–956.
30. R. G. WISSINGER and M. E. PAULAITIS, *ibid.* **25** (1987) 2497–2510.
31. G. K. FLEMING and W. J. KOROS, *ibid.* **28** (1990) 1137–1152.
32. S. M. JORDAN, G.K. FLEMING and W. J. KOROS, *ibid.* pp. 2305–2327.
33. B. J. BRISCOE and S. ZAKARIA, *J. Mater. Sci.* **25** (1990) 3017–3023.
34. A. N. GENT and P. B. LINDLEY, *Proc. Royal Soc. London*, Series A. Mathematical and Physical Sciences **249** (1959) 195–205.
35. M. L. WILLIAMS and R. A. SCHAPERY, *Int. J. Fracture Mech.* **1** (1) (1965) 64–72.
36. G. H. LINDSEY, *J. Appl. Phys.* **38** (12) (1967) 4843–4852.
37. A. N. GENT and D. A. TOMPKINS, *J. Polym. Sci.: Part A-2* **7** (1969) 1483–1488.
38. A. N. GENT and D. A. TOMPKINS, *J. Appl. Phys.* **40** (6) (1969) 2520–2525.
39. B. J. BRISCOE and S. ZAKARIA, *Polymer* **31** (1990) 440–447.
40. B. J. BRISCOE and S. ZAKARIA, *J. Polym. Sci.: Part B, Polym. Phys.* **30** (1990) 959–969.
41. A. N. GENT and Y. C. HWANG, *J. Mater. Sci.* **25** (1990) 4981–4986.
42. A. N. GENT and C. WANG, *ibid.* **26** (1991) 3392–3395.
43. M. R. HOLL, Dynamic analysis, measurement, and control of cell growth in solid state polymeric foams, University of Washington, 1995.
44. E. E. UNDERWOOD, "Quantitative Stereology," (Addison-Wesley, Reading Massachusetts, 1970).

Received 27 January 1997
and accepted 2 April 1998